Clara M. Ionescu, Dana Copot, and Cristina Muresan

A multi-scale model of nociception pathways and pain mechanisms

Abstract: To develop suitable pain management policies and drug delivery assist devices for analgesia (i. e., pain alleviation), it is necessary to have a mathematical model which captures the essential dynamics of this complex process. Recent work points to the fact that pain can be characterized by several dynamic stages, including anomalous diffusion and spatio-temporal dependency on tissue characteristics. This chapter presents a physiologically based mathematical framework to capture nociceptor pathways and pain reception, transmission and perception, in the human body. The main difference with previous studies is the explicit incorporation of fractional calculus tools as a natural way to characterize biological phenomena. Next, we observe the effects in skin impedance in the presence of nociceptor stimulation. For this purpose, a prototype device has been carefully designed to allow for the application of a non-invasive measurement protocol. Bio-electrical skin impedance captures the changes in tissue content at various time instants, sensor locations, and stimulus trains. The existence of a memory effect – or residual pain – is observed from the data.

Keywords: Nociceptor pathway, chronic pain, analgesia, bio-impedance, fractional-order impedance models, non-invasive measurement, mathematical model, residual pain, memory

MSC 2010: 65D30, 92C30, 92C50, 93A30, 93B30, 93C10, 93C80, 93C95, 97M10

1 Introduction

Pain is rather a subjective and personal sensation, especially in awake and aware individuals [26, 40]. The self-evaluation metrics often become biased by the tissue memory, i. e., perception of pain in its absence, or artificially elevated levels of pain due to

Acknowledgement: This chapter has been financially supported by Flanders Research Center, grant nr. G026514N and G008113N, and post-doctoral fellowship grant nr. 12B3415N (C. M. Ionescu). Part of this work has been carried out within COST Action CA15225, a network supported by COST (European Cooperation in Science and Technology).

Clara M. Ionescu, Dana Copot, Department of Electrical energy, Metals, Mechanical Constructions and Systems, Research group on Dynamical Systems and Control, Ghent University, Technologiepark 914, 9052 Ghent Zwijnaarde, Belgium, e-mails: claramihaela.ionescu@ugent.be, dana.copot@ugent.be
Cristina Muresan, Department of Automation, Technical University of Cluj Napoca, Memorandumului nr 28, Cluj, Romania, e-mail: cristina.muresan@aut.utcluj.ro

https://doi.org/10.1515/9783110571905-004

anxiety, discomfort, and fear [7]. The most frequently used tools to assess acute pain are the numeric rating scale (NRS) and the visual analog scale (VAS), ranging from 0 (no pain) to 10 (excessive pain), e. g., by means of the Wong–Baker faces scale.

However, many critically ill patients are unable to communicate effectively because of cognitive impairment, sedation, paralysis, or unconsciousness (e. g., due to general anesthesia). Another group unable to communicate pain are neonates and infants [12]. As such, no single tool is universally accepted for use in the non-communicative (anesthetized) patient [20, 16]. When a patient cannot express himself, observable indicators – both physiologic and behavioral – have been treated as pain-related indicators to evaluate the pain level [14]. Thus the numbers are simply estimates of the perception of the pain, based on past personal experience of the caregiver.

The state of absence of pain due to medication is referred to as *analgesia*. It is important to admit that patient analgesic needs can differ depending on clinical circumstances, and that for any given patient therapeutic targets are likely to change over time, mainly due to drug trapping [4]. Thus, achieving patient comfort and ensuring patient safety, including avoidance of over- and under-dosage, relies on accurately measuring pain, agitation, sedation, and other related variables. This should be evaluated with validated tools that are easy to use, precise, accurate, and sufficiently robust to include a wide range of behaviors. From the point view of analgesia and chronic pain management, the community is still missing an adequate pain measurement tool based on objective processing of information. A comprehensive review of available tools to extrapolate on pain levels is given in [2].

A linear input-output-based model was identified by performing thermal cold stimuli into dental nerves and measuring the resulting electrical activity correlated to pain [9]. The model was a simple second-order transfer function with damping factor and impulse response corresponding to measured electrical activity in interdental nerves. This crude model was further improved to better approximate the intra-patient variability and plasticity of pain sensation after repeated stimuli [8]. Further in vivo tests indicated that modulation is present in the electrical activity when pain is perceived by the subject, suggesting thus that a frequency dependence is necessary. Non-linear terms in sine and cosine functions have been introduced in [10] to predict this non-linear effect.

Somewhat later, a review of multi-scale processes involved in nociception and pain sensation has been made, summarizing all steps from thermal stimuli [45]. Although the review provides an excellent overview, it concludes that the mechanistic processes are far from being well understood and that engineering tools need to be further employed for delivering useful models for assessing pain in humans. A model for electrical activity aroused from thermal nociceptor detection and transmission at the neuronal level is then given. Later studies on thermal pain indicated the presence of adaptability and variability in pain sensation as a result of the noxious stimulus intensity degree and the pattern of stimulation [27]. In engineering terms, this

s due to variability of disturbance profiles (i. e., stimuli) and thus the excitatory in-ıut to the measured response variation provides a spatio-temporal change in the ıathway. Simple linear models of classical system engineering theory can no longer apture such changes without increasing the complexity of the problem formula-ion.

2 Physiological background

The detection of stimuli that are capable of producing tissue injury is termed noci-ception. These primary sensory neurons have cell bodies in the dorsal root ganglia or in the trigeminal ganglia and possess naked peripheral endings that terminate in the skin, mostly in the epidermis (upper layer of the skin) [33]. Nociceptors, the re-ceptors of pain, are the first unit in the series of neurons related to nociceptive pain. They transduce mechanical, chemical, and thermal energy into ionic current (noxious stimuli result in depolarizations that generate action potentials), conduct the action potentials from the peripheral sensory neurons to the central nervous system (CNS), and convert the action potentials into neurotransmitter release at the presynaptic ter-minal [33].

In peripheral nerves, nociceptors have unmyelinated (C-fibres) or thinly myeli-nated ($A\delta$-fibres) axons [25]. Nociceptors have a lower conduction velocity compared to other peripheral sensory nerve fibres. Generally, the $A\delta$-fibres have a medium diameter of 2–6 μm with a conduction velocity of 12–30 m/s. In comparison, the C-fibres have a small diameter of 0.4–1.2 μm with a conduction velocity of 0.5–2 m/s. These types of fibres account for the fast and slow pain responses, respectively. Of another type of fibres, the large-diameter $A\beta$-fibres, the conduction velocity is about 30–100 m/s.

According to the response to different stimuli, nociceptors can be further classified as high-threshold mechanoreceptors, chemoreceptors, temperature-sensitive recep-tors (heat/cold), polymodal nociceptors, and mechano-insensitive (silent) nocicep-tors. About 70 % of the $A\delta$-fibre nociceptors are mechanical, 20 % are mechano-heat, and 10 % are mechanic-cold nociceptors [25].

Ion channels in the plasma membrane of nociceptors have a key role in the trans-duction of stimuli; these are proteins located in the cell membrane that selectively me-diate the transmembrane transportation of specific ions or molecules. The ion chan-nels include heat activated channels, capsaicin receptor-dependent channels, adeno-sine triphosphate (ATP)-gated channels, proton-gated channels, nociceptor-specific voltage-gated $NA+$ channels, and mechano-sensitive channels.

All these types of channels are essentially converted from closed to open states by mainly three types of stimulus: thermal (threshold 43 °C), mechanical (threshold 0.2 MPa), and chemical. The voltage-gated channels are the most important. These

respond to membrane depolarization or hyperpolarization and are substantial to the generation and transmission of electrical signals along axons. When a noxious stimulus reaches a nociceptor, the corresponding ion channels will be opened, which will induce a transmembrane current and increase the membrane voltage. When this voltage increases to the threshold, specified sodium channels will open in a positive feedback mode that results in the depolarization of the membrane, eventually generating an action potential.

Primary afferent nociceptors mostly terminate in the spinal cord, which has an important role in the integration and modulation of pain-related signals. Second-order neurons receiving input from nociceptors and projecting to the brain are located in both superficial and deep laminae of the dorsal horn [25]. These cells often have convergent inputs from different sensory fibre types and different tissues. Both pre- and post-synaptic elements are strongly gated by descending excitatory and inhibitory influences from the brain. The inhibitory influences use neurotransmitters that are mimicked by some analgesic drugs.

During consciousness, using MRI, it is possible to identify those brain areas directly related to pain [25, 24]. Such a stimulus reliably leads to activation of multiple brain areas, jointly termed the pain matrix. Different areas represent different aspects of pain. The primary and secondary somatosensory cortices are activated to discriminate the location and intensity of a painful stimulus. The anterior cingulate cortex, frontal cortex, and anterior insula regions may be related to the cognitive and emotional components. The problem is that these areas show significant modulation depending on the context of the stimulus, e. g., degree of attention, anxiety, expectation, depression, and analgesic drug treatment.

There is an established relation between the nociceptor pathway and dynamics of potassium channels, i. e., the sodium–potassium pump, for signaling between intracellular fluid and extra-cellular fluid (ECF) in the biological tissue [33]. The observed increase in potassium concentration in the ECF varies between 0.1 and 10.0 mmol/L and depends on stimulation frequency, intensity, and duration [25]. In vitro validation studies have been performed to verify the use of the proposed models for detecting changes in the concentration of these cations in controlled environment solutions [3].

From this initial step, we extrapolated that one may measure non-invasively the changes in the signaling pathways, by means of bio-electrical impedance, via the skin [43]. The proposed method for measurement is based on sending an excitatory electrical signal to the skin, while measuring its response as voltage and current changes. By changing the signaling conditions (i. e., with mechanical nociceptor stimulation) the impedance so measured changes its values as well, as a result of changes in the composition of the intra-cellular fluid and the ECF by the movement of the cations.

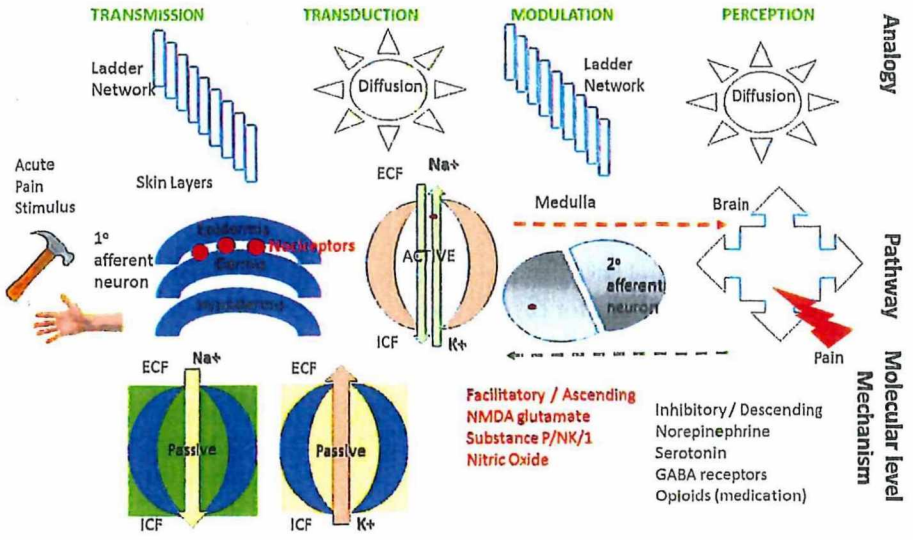

Figure 1: Schematic overview of main sequences in nociceptor pathways and model rationale equivalent.

3 Multi-scale model development

Originating from our prior work on modelling biological tissue with fractional-order impedance models (FOIMs), the following extension is proposed. An overview of the processes and equivalence to model development is depicted in Figure 1, including changes at the molecular level.

The physiological pathway of pain can be described as four main processes [33]:

- transduction – when a stimulus is applied to the skin, the nociceptors located there trigger action potentials by converting the physical energy from a noxious thermal, mechanical, or chemical stimulus into electrochemical energy;
- transmission – the signals are subsequently transmitted in the form of action potentials (similar to pulse trains) via nerve fibers from the site of transduction (periphery) to the dorsal root ganglion or the trigeminal ganglion, which then activates the interneuron;
- perception – the appreciation of signals arriving in specified areas in the cerebral cortex as pain; and
- modulation – descending inhibitory and excitatory input from the brainstem that influences (modulates) nociceptive transmission from the spinal cord.

The stimulatory effects of nociception are essentially considered an ultra-capacitor, which is represented by a non-rational form of a transfer function model in $(j\omega)^n$, with n being any real number [31, 11]. Specifically, the skin–electrode interface, the

stratum corneum, and ionic pathways can be modeled as elements in an electrical network. Various models describe this interface using constant or current-dependent resistive-capacitive equivalent circuits [39, 32, 15, 13]. Using fraction expansion theory, a lumped FOIM can be obtained as a fractional-order integral [19]. Similarly, *transmission* in signaling pathways occurs via neuronal activity, already modeled with FOIMs from resistance-inductance equivalent electrical network elements [17], expressed by a fractional-order derivative.

The perception model based on combined exponential and power law functions seems to be a good candidate for capturing essential electrical activity modulated in the brain [1]. Plasticity in synaptic variance is introduced in a layer-based sensory area in the cortex by reverse node engineering modeling [37]. In the case of pain perception, the combined effect can be obtained by using the Mittag-Leffler function, which is well known to capture hybrid exponential and power law behavior in biological tissues [24, 41].

Diffusion of perception sensory activity in the brain using the Mittag-Leffler function in the time domain corresponds to a non-integer-order derivative easily expressed in the frequency domain [44]. Layered activity can be represented by ladder networks with serial connection of RC cells. To account for plasticity, the RC cells are not identical; instead they behave as a memristor with unbalanced dynamics. For instance, it is expected that the first pain perception is more intense than the second, given the latency of the delayed pain stimulus (i. e., sharp first increase followed by slowly decaying tail).

Assuming the brain cortex area to be a porous tissue whose porosity varies (i. e., intra- and extra-cellular space tissue with different densities), one can model the changes in viscosity as a function of this porous density. It has been shown that fractional-order derivatives are natural solutions to anomalous diffusion equations [19, 24, 44, 28]. The use and physical interpretation of this very useful fractional calculus tool has been discussed in several works, e. g., [24, 30, 21, 22, 18]. The net advantage of using the Mittag-Leffler function is that it allows for the introduction of memory formalism [38], therefore taking into account the tissue rheology. The mixed area in brain tissue will introduce a dynamic viscosity and thus a dynamic perception of nociceptor-induced pain [42, 23]. Finally, the perception and modulation activity can be characterized yet again by an FOIM as differ-integral (depending on the sign of the non-rational order) [44, 36].

In conclusion, a lumped FOIM comprising the main processes described above is given by

$$Z_{\mathrm{FOIM}}(s) = R + \frac{\mathrm{TD}}{s^{\alpha_1}} + \frac{\mathrm{TS}}{s^{\alpha_2}} + Ps^{\alpha_3}, \tag{1}$$

where $\alpha_1, \alpha_2, \alpha_3 \in (-1, 0) \cup (0, 1)$ and TD denotes transduction, TS denotes transmission, and P denotes perception. A calibration factor has been added, a gain R. It may be that not all terms in this model are necessary at all times, as some of the physiological

rocesses may be impaired in some applications (e. g., analgesia will fix the effect of ıe perception term in P at zero) [5]. The units are arbitrary, as the model is defined as difference to the initial state of the patient – due to the use of fractional derivatives – nd not as absolute values. This enables patient specificity since no generic model is ssumed to be valid and thus broadcasts a new light upon the interpretation of such ıodels.

4 Preliminaries

'igure 2 depicts the flowchart of the measurement protocol. For this purpose, a proto-ype device has been developed, ANSPEC-PRO, depicted in Figure 3, and the electrode s placed in the hand palm.

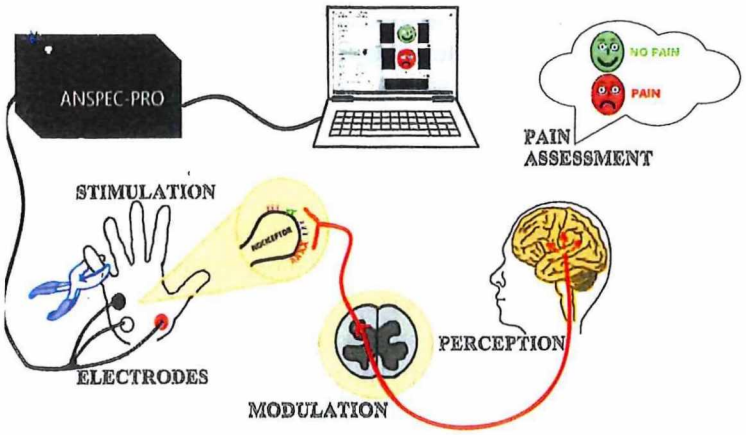

Figure 2: Flowchart of the measurement process.

Figure 3: Left: The ANSPEC-PRO prototype for non-invasive measurement of bio-electrical skin impedance. Right: Placement of the electrodes during proof-of-concept measurements; two current carrying electrodes (white, red) and one pick-up electrode (black).

The measurement flowchart can be summarized as follows:

- design a multi-sine signal with 29 components in the frequency interval 100–1500 Hz, with step interval of 50 Hz; the multi-sine signal is sent with an amplitude of 0.2 mA, a factor 5 below the maximum allowed by clinical standards [6];
- send this signal and acquire the measured signals at sampling frequency of 15 KHz;
- use a 3M three-point electrode sensor in the hand palm (CE-marked) (according to MDD93/42/EEC);
- measure current and voltage via a National Instruments (Texas, USA) device (cRIO9074 with NI9201- and NI9263-slots);
- store the signals online or on the computer for further processing.

The computer is a laptop with the operating system Windows 7 Enterprise 64-bit and an INTEL(R) Core(TM) i7-6600U CPU@2.80GHz processor. A graphical user interface allows monitoring of signal quality.

The measurement requires three-point electrodes: two current carrying electrodes and one pick-up electrode. The latter measures the voltage without carrying any currents; hence, no polarization occurs. All electrodes were placed on the palmar side of the hand (see Figure 3). A calibration of the measurements was performed for each volunteer by measuring for 10 minutes without nociceptor stimulus applied and without removing the electrodes.

The study was carried out on one healthy volunteer, without pain relief medication treatment at the measurement moment. In this individual, two consecutive measurements were executed to investigate the repeatability and existence of pain memory. Sensors were placed on the right hand and the nociceptor stimulation was applied at the same location (i. e., the same hand). The protocol summarized in Table 1 was applied.

Table 1: The time intervals and actions within the 10-minute measurement protocol. The P/NP denote the acronym used in the figures to indicate the case.

Time interval (min)	Nociceptor stimulation
0–2	Absent (NP1)
2–3	Present (P1)
3–6	Absent (NP2)
6–7	Present (P2)
7–10	Absent (NP3)

The measured signals are filtered for noise prior to the application of non-parametric identification methods [29]. Given the input is of sinusoidal type ($A\sin(\omega t)$), the

ıpedance is a frequency-dependent complex variable evaluated as

$$Z(j\omega) = \frac{S_{XX}(j\omega)}{S_{XY}(j\omega)}, \tag{2}$$

here $S_{XX}(j\omega)$ denotes the auto-correlation spectrum of the signal, $S_{XY}(j\omega)$ denotes e cross-correlation spectra between the input-output signals, $\omega = 2\pi f$ is the an- ılar frequency in rad/s, with f being the frequency in Hz, and $j = \sqrt{-1}$. The clas- cal periodogram filtering technique has been applied with no overlapping interval, ith windowing function Blackman implemented in the Matlab environment [29]. The ıpedance is then evaluated every minute from online data streaming and plotted ;ainst frequency. This is then a frequency response either in complex form (real and ıaginary parts), or in Bode plot form (magnitude and phase).

Results and discussion

ıe time-based current and voltage signals were acquired at a sampling frequency of ; kHz. A snapshot of a small interval is depicted in Figure 4. In this figure one observes ıe input signal (current) remains the same at all times, while the recorded output gnals (skin response) undergoes changes between the NP and P intervals (recall the rotocol from Table 1).

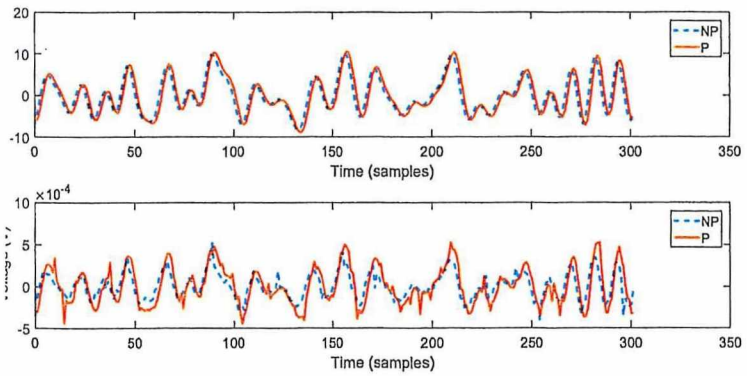

gure 4: Time-based input-output signals for a snapshot of the interval with absent (NP)/present (P) ociceptor stimulation.

ıe frequency response of the complex impedance calculated using (2) and illustrated y means of changes with respect to calibrated impedance prior to the test is depicted ı Figure 5 for one individual test. In this figure one may observe the following:

- applying the same mechanical nociceptor stimuli, the real part of the impedance decreases from P1 to P2, i. e., the level of perception of the pain is lower;

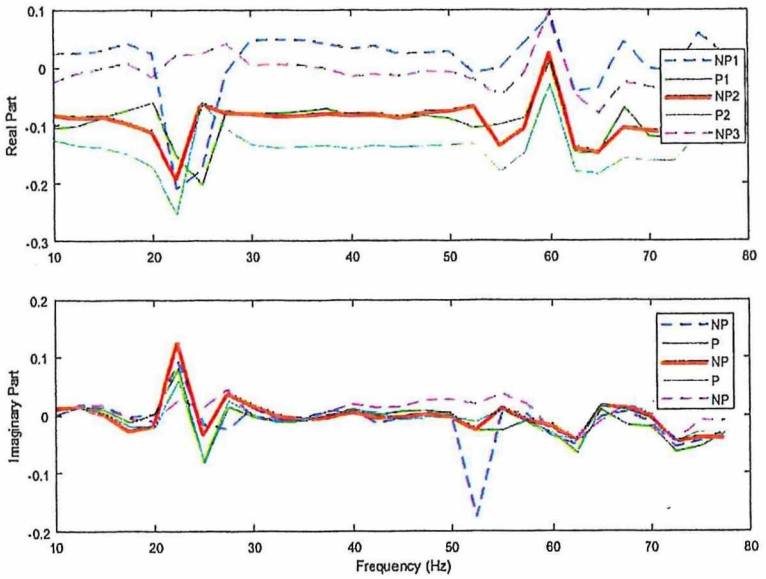

Figure 5: Changes in impedance as a function of frequency by means of its real and imaginary parts, calculated per interval of absent (NP)/present (P) nociceptor stimulation.

– the impedance values during absence of nociceptor stimulation decrease from one interval NP1 to another, i. e., NP2, NP3, while NP2 overlaps with P1, i. e., the memory of the stimulation persists in the tissue.

For the same individual, for the pain P1 interval, the fitting of the FOIM from (1) onto the frequency response complex impedance data is depicted in Figure 6. The fitting was again obtained using non-linear least squares identification, with steepest gradient descent, in an iterative manner. Iteration was performed to avoid local minima and

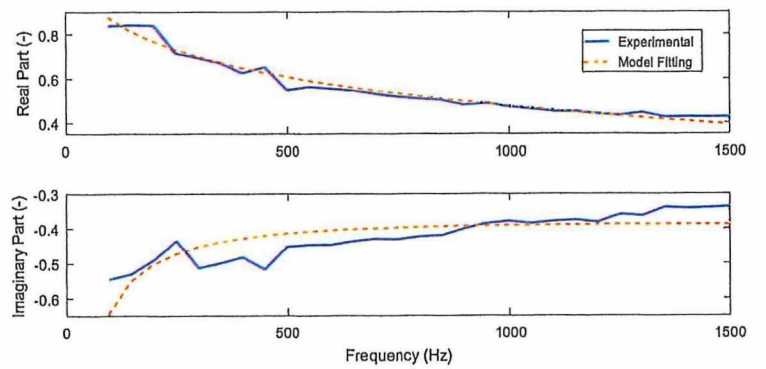

Figure 6: Identified FOIM for the raw impedance data P1.

ıe number of iterations between the identified results varied between #2 and #4 in all ata. The iteration was stopped when the model parameters changed less than 5 %.

It is important to understand that the method and models developed here are niquely defined for each individual. In other words, the reporting of the model values ı not relevant here because the data are expressed with respect to the initial moment f measurement, whereas the state of the patient is taken as a reference. Hence, all alues reported are in fact calibrated for that reference value of impedance and each ıdividual has his/her own initial state values.

The use of FOIMs is now justified by the data in some sense that, indeed, tissue ıemory exists and it is a feature naturally explained with properties of mathematical ıodels from fractional calculus. The detailed description of properties of FOIMs has een given in numerous other reports, hence it is omitted here [24, 30].

The data are nevertheless relevant, for they support a method, a device, and mathmatical models to provide an indication of change in bio-electrical impedance meaured via skin electrodes correlated with absence/presence of nociceptor stimulation. 'his is a first step towards developing a full measurement set-up and an algorithm for ıuantifying related pain levels.

Our proposed tools are in the same line of thought as those presented in [34, 35]. ۱n intelligent analysis system based on fuzzy logic models was successfully tested in ɔost-operative patients, whereas patient-controlled analgesia (morphine-based) was itrated from the determined index. With respect to their work, our work differs in that t delivers a mathematical framework related to the actual tissue dynamics (i. e., memɔry, dielectric) properties and thus justifies the use of FOIMs.

The changes in the skin impedance affect both time and frequency domains, as ɜuggested by our results reported in this chapter. These changes are evaluated with reɜpect to an initial state of the individual, e. g., when it experiences no pain or when the evel of pain is already characterized via other assessment tools (verbal or non-verbal, lepending on the state of the patient). It should be noted that in certain situations, ɔare must be taken when referencing to other states of the patient. For instance, if the ɒainless state is recorded before a surgical intervention involving general anesthesia ɔf the patient, the composition of the interstitial tissue will be greatly affected by the ɔocktail of medication given during this intervention. Following ICU evaluation, pain levels will then have to be referenced to a more recent state of the patient. However, if the pain assessment is to be performed during the surgical nociceptor stimulation, then the referencing with the pre-operatory state of the patient may be relevant.

The present study is limited in the number of individuals measured. No actual chronic pain patients or ICU post-operatory pain patients have been included. A correlation to clinical practice indices, such as the Wong–Baker faces scale, should be investigated using a larger population in order to extract a mathematical relationship between model parameters and clinical levels of pain. Although the method is personalized, i. e., the values are calibrated to the initial state of the individual/patient, an analysis of the influence of BMI on the accuracy of the estimators should also be

performed. We do not claim the values given here are reference values. Rather, they are specific for the individual included in this study.

6 Conclusions

This chapter introduced a physiological and mathematical framework to allow understanding the pain mechanism and detect the nociception stimulation effects in skin impedance in a healthy volunteer as a proof of concept. The notoriously successful FOIM formulation has proven once more useful to characterize time and frequency evolution of a pre-defined protocol of nociceptor stimulation applied non-invasively in one subject.

The next steps are an in-depth analysis in post-operatory patients under pain alleviation treatment and correlations to standard clinical practice of pain level assessments.

Bibliography

[1] R. Bogacz, A tutorial on the free-energy framework for modelling perception and learning, *J. Math. Psychol.*, **76** (2017), 198–211.

[2] D. Copot, *Fractional Order Tools for Characterising Diffusion in the Human Body*, Doctoral Thesis, Ghent University, 2018.

[3] D. Copot, R. De Keyser, and C. M. Ionescu, Identification and performance analysis of fractional order impedance model for various test solutions, in *Int. Conf. on Fractional Differentiation and Its Applications, NoviSad, Serbia*, pp. 542–550, 2016.

[4] D. Copot, R. Magin, R. De Keyser, and C. M. Ionescu, Data-driven modelling of drug tissue trapping using anomalous kinetics, *Chaos Solitons Fractals*, **102** (2017), 441–446.

[5] N. D. Crosby, C. L. Weisshaar, J. R. Smith, M. Zeeman, M. Goodman-Keiser, and B. Winkelstein, Burst and tonic spinal cord stimulation differentially activate GABAergic mechanisms to attenuate pain in a rat model of cervical radiculopathy, *IEEE Trans. Biomed. Eng.*, **62**(6) (2015), 1604–1613.

[6] R. Fish and L. Geddes, Conduction of electrical current to and through the human body: a review, *OA J. Plast. Surg. (ePlasty)*, **9** (2009), 407–421.

[7] E. Flaherty, Using pain-rating scales with older adults, *Am. J. Nurs.*, **108**(6) (2008), 40–47.

[8] U. G. Fors, M. L. Ahlquist, G. A. Edwall, and G. A. Haegerstam, Evaluation of a mathematical model analysing the relation between intradental nerve impulse activity and perceived pain in man, *Int. J. Bio-Med. Comput.*, **19** (1986), 261–277.

[9] U. G. Fors, M. L. Ahlquist, R. Skagerwall, G. A. Edwall, and G. A. Haegerstam, Relation between intradental nerve activity and estimated pain in man – a mathematical model, *Pain*, **18** (1984), 397–408.

[10] U. G. Fors, G. A. Edwall, and G. A. Haegerstam, The ability of a mathematical model to evaluate the effects of two pain modulating procedures on pulpal pain in man, *Pain*, **33** (1988), 253–264.

[11] C. Gabriel, S. Gabriel, and E. Corthout, The dielectric properties of biological tissues: I. Literature survey, *Phys. Med. Biol.*, **41** (1996), 2231–2249.
[12] B. Gholami, W. Haddad, and A. R. Tannenbaum, Relevance vector machine learning for neonate pain intensity assessment using digital imaging, *IEEE Trans. Biomed. Eng.*, **57**(6) (2010), 1457–1466.
[13] G. F. Goddard, A pilot study of the changes of skin electrical conductance in patients undergoing general anaesthesia and surgery, *Anaesthesia*, **37**(4) (1982), 408–415.
[14] T. Hadjistavropoulos, D. Chapelle, H. Hadjistavropoulos, S. Green, and G. Asmundson, Using facial expressions to assess musculoskeletal pain in older persons, *Eur. J. Pain*, **6**(3) (2002), 179–187.
[15] K. E. Hagbarth, R. G. Hallin, A. Hongell, H. E. Torebjörk, and B. G. Wallin, General characteristics of sympathetic activity in human skin nerves, *Acta Physiol. Scand.*, **84**(2) (1972), 164–176.
[16] K. Herr, P. Coyne, T. Key, R. Manworren, M. McCaffery, S. Merkel, J. Pelosi, and L. Wild, Pain assessment in the non-verbal patient: Position statement with clinical practice recommendations, *Pain Manag. Nurs.*, **7**(2) (2006), 44–52.
[17] C. M. Ionescu, The phase constancy in neural dynamics, *IEEE Trans. Syst. Man Cybern., Part A, Syst. Hum.*, **42**(6) (2012), 1543–1551.
[18] C. M. Ionescu, A memory-based model for blood viscosity, *Commun. Nonlinear Sci. Numer. Simul.*, **45** (2017), 29–34.
[19] C. M. Ionescu, A. Lopes, D. Copot, J. A. Tenreiro Machado, and J. H. T. Bates, The role of fractional calculus in modelling biological phenomena: a review, *Commun. Nonlinear Sci. Numer. Simul.*, **51** (2017), 141–159.
[20] J. Jacobi, G. Fraser, D. Coursin, R. Riker, D. Fountaine, E. T. Wittbrodt, D. B. Chalfin, M. F. Masica, H. S. Bjerke, W. M. Coplin, D. W. Crippen, B. D. Fuchs, R. M. Kelleher, P. E. Marik, S. A. Nasraway, M. J. Murray, W. T. Peruzzi, and P. D. Lumb, Clinical practice guidelines for the sustained use of sedatives and analgesics in the critically ill adult, *Crit. Care Med.*, **30**(1) (2002), 119–141.
[21] Y. Li, Y.-Q. Chen, and I. Podlubny, Mittag-Leffler stability of fractional order nonlinear dynamic systems, *Automatica*, **45**(8) (2009), 1965–1969.
[22] Y. Li, Y.-Q. Chen, and I. Podlubny, Stability of fractional-order nonlinear dynamic systems: Lyapunov direct method and generalized Mittag–Leffler stability, *Comput. Math. Appl.*, **59**(5) (2010), 1810–1821.
[23] B. Lundstrom, M. Higgs, M. William, W. Spain, and A. Fairhall, Fractional differentiation by neocortical pyramidal neurons, *Nat. Neurosci.*, **11** (2008), 1335–1342.
[24] R. Magin, B. Vinagre, and I. Podlubny, Fractional calculus in bioengineering, *IEEE Syst. Man Cybern. Mag.*, **July** (2018), 23–28.
[25] S. McMahon, M. Koltzenburg, I. Tracey, and D. Turk, *Wall and Melzack's Textbook of Pain*, Elsevier Saunders, 2013.
[26] R. Melzack, From the gate to the neuromatrix, *Pain*, **82** (1999), S121–S126.
[27] C. D. Morch, K. S. Frahm, R. C. Coghill, L. Arendt-Nielsen, and O. K. Andersen, Distinct temporal filtering mechanisms are engaged during dynamic increases and decreases of noxious stimulus intensity, *Pain*, **156** (2015), 1906–1912.
[28] C. Nicholson, Diffusion and related transport properties in brain tissue, *Rep. Prog. Phys.*, **64** (2001), 815–884.
[29] R. Pintelon and J. Schoukens, *System Identification: A Frequency Domain Approach*, Wiley, IEEE, 2005.
[30] I. Podlubny, Geometric and physical interpretation of fractional integration and fractional differentiation, *Fract. Calc. Appl. Anal.*, **5**(4) (2002), 367–386.
[31] C. S. Poon and T. Choy, Frequency dispersions of human skin dielectrics, *Biophys. J.*, **34** (1981), 135–147.

[32] I. Roeggen, H. Storm, and D. Harrison, Skin conductance variability between and within hospitalised infants at rest, *Early Hum. Dev.*, **87**(1) (2011), 37–42.
[33] J. Schuttler and H. Schwilden, *Modern Anesthetics*, Springer, Berlin, Heidelberg, 2008.
[34] J. S. Shieh, C. Y. Dai, Y. Wen, and W. Z. Sun, A novel fuzzy pain demand index derived from patient-controlled analgesia for postoperative pain, *IEEE Trans. Biomed. Eng.*, **54**(12) (2007), 2123–2132.
[35] J. S. Shieh, M. Fu, S. J. Huang, and M. C. Kao, Comparison of the applicability of rule-based and self-organizing fuzzy logic controllers for sedation control of intracranial pressure pattern in a neurosurgical intensive care unit, *IEEE Trans. Biomed. Eng.*, **53**(8) (2006), 1700–1705.
[36] D. Sierociuk, T. Skovranek, M. Macias, I. Podlubny, I. Petras, A. Dzielinski, and P. Ziubinski, Diffusion process modeling by using fractional-order models, *Appl. Math. Comput.*, **257** (2015), 2–11.
[37] G. Tononi, An information integration theory of consciousness, *BMC Neurosci.*, **5** (2004), 42 pp.
[38] J. Trujillo, Fractional models: Sub and super-diffusives, and undifferentiable solutions, in *Innovation in Engineering Computational Technology*, pp. 371–401, 2006.
[39] J. L. Vargas Luna, M. Krenn, J. A. Cortes Ramirez, and W. Mayr, Dynamic impedance model of the skin-electrode interface for transcutaneous electrical stimulation, *PLoS ONE*, **10**(5) (2015), e0125609.
[40] P. Wall and R. Melzack, *The Challenge of Pain*, Penguin, London, United Kingdom, 1996.
[41] B. West, Fractal physiology and the fractional calculus: a perspective, *Front. Physiol.*, (2010) 10.3389/fphys.2010.00012.
[42] D. Wheatley, Diffusion theory, the cell and the synapse, *BioSystems*, **45** (1998), 151–163.
[43] Y. Yang, F. Zhang, K. Tao, L. Wang, H. Wen, and Z. Teng, Multi-frequency simultaneous measurement of bioimpedance spectroscopy based on low crest factor multisine excitation, *Physiol. Meas.*, **36**(3) (2015), 489–501.
[44] X. J. Zhou, Q. Gao, O. Abdullah, and R. L. Magin, Studies of anomalous diffusion in the human brain using fractional order calculus, *Magn. Reson. Med.*, **63**(3) (2010), 562–569.
[45] Y. J. Zhu and T. J. Lu, A multi-scale view of skin thermal pain: from nociception to pain sensation, *Philos. Trans. R. Soc. A*, **368** (2010), 521–559.